Disconnection in a left-hemispheric temporo-parietal network impairs multiplication fact retrieval

Stefan Smaczny, Christoph Sperber, Stefanie Jung, Korbinian Möller, Hans-Otto Karnath, Elise Klein

S. Smaczny[1], C. Sperber[2], S. Jung[3,4], K. Moeller[4,5,6], H.-O. Karnath[1,7 †] & E. Klein[4,8 †]

1: Centre of Neurology, Division of Neuropsychology, Hertie-Institute for Clinical Brain Research, University of Tuebingen, Tuebingen, Germany; 2: Department of Neurology, Inselspital, University Hospital Bern, University of Bern, Bern, Switzerland; 3: Department of Computer Science/Therapy Science, Trier University of Applied Science, Trier, Germany; 4: Leibniz Institut fuer Wissensmedien, Tuebingen, Germany; 5: Centre for Individual Development and Adaptive Education of Children at Risk (IDeA), Frankfurt, Germany; 6: Centre for Mathematical Cognition, School of Science, Loughborough University, United Kingdom; 7: Department of Psychology, University of South Carolina, Columbia, SC; 8: University of Paris, LaPsyDÉ, CNRS, Sorbonne Paris Cité, Paris, France

[†] Shared Correspondence (karnath@uni-tuebingen.de; elise.klein@u-paris.fr).

Disconnection in a left-hemispheric temporo-parietal network impairs multiplication fact retrieval

Abstract

Arithmetic fact retrieval has been suggested to recruit a left-lateralized network comprising perisylvian language areas, parietal areas such as the angular gyrus (AG), and non-neocortical structures such as the hippocampus. However, the underlying white matter connectivity of these areas has not been evaluated systematically so far.

Using simple multiplication problems, we evaluated how disconnections in parietal brain areas affected arithmetic fact retrieval following stroke. We derived disconnectivity measures by jointly considering data from n=73 patients with acute unilateral lesions in either hemisphere and a white-matter tractography atlas (HCP-842) using the Lesion Quantification Toolbox (LQT). Whole-brain voxel-based analysis indicated a left-hemispheric cluster of white matter fibers connecting the AG and superior temporal areas to be associated with a fact retrieval deficit. Subsequent analyses of direct grey-to-grey matter disconnections revealed that disconnections of additional left-hemispheric areas (e.g., between the superior temporal gyrus and parietal areas) were significantly associated with the observed fact retrieval deficit.

Results imply that disconnections of parietal areas (i.e., the AG) with language-related areas (i.e., superior and middle temporal gyri) seem specifically detrimental to arithmetic fact retrieval. This suggests that arithmetic fact retrieval recruits a widespread left-hemispheric network and emphasizes the relevance of white matter connectivity for number processing.

Keywords

Disconnectome, VLSM, Arithmetic Fact Retrieval, Lesion Mapping, Connectivity

Highlights

- Examination of the effect of disconnectivity following stroke on multiplication
- WM between AG and superior temporal areas was associated with worse multiplication
- Disconnections in the arithmetic fact retrieval network led to worse multiplication
- White matter disconnectivity needs more examination in numerical cognition research

1. Introduction

The dominating view in numerical cognition is that arithmetic facts such as multiplication tables are stored in and retrieved from long-term memory in a verbal format (e.g., Dehaene et al., 2003; Delazer et al., 2003; Grabner et al., 2009). The triple code model (Dehaene & Cohen, 1995; 1997; Dehaene et al., 2003), which has been remarkably successful in providing a theoretical framework for neuroimaging research on numerical cognition, posits that the retrieval of arithmetic facts recruits areas also involved in language processing such as left-hemispheric perisylvian areas and the left angular gyrus (AG). In contrast, the manipulation of numerical content during magnitude-manipulation-based calculation (e.g., addition, subtraction) has been associated with a fronto-parietal network for number (magnitude) processing centered around the intraparietal sulcus (IPS; e.g., Dehaene et al., 2003; for a meta-analysis see Arsalidou & Taylor, 2011). This network has recently been coined the 'math-responsive network' (Amalric & Dehaene, 2017; 2019).

The retrieval of rote learned arithmetic facts has been assumed to be processed multi-modularly and distributed within a left-lateralized language network, including inferior frontal gyrus (IFG; Delazer et al., 2003), middle and superior temporal gyri (MTG/STG), supramarginal gyrus (SMG), intraparietal sulcus (IPS, Salillas et al, 2011); angular gyrus (AG; e.g., Dehaene et al., 2003; Delazer et al., 2003; Grabner et al., 2009a; 2009b), and hippocampus (e.g., Bloechle et al., 2016; Delazer et al., 2019; Klein et al., 2016; 2019). However, it is important to note that recent evidence in healthy participants and from neurosurgery in tumor patients has also pointed to the role of right hemispheric structures in tasks reliant on arithmetic fact retrieval (Arcara et al., 2021; Salillas et al, 2021; Semenza et al., 2017). However, the exact role of some of these areas is still debated. On the one hand, several case studies reported patients with a preserved AG who presented selective deficits for arithmetic fact retrieval (as measured by a multiplication task, Cohen et al., 2000; Dehaene & Cohen, 1997; Van Harskamp et al., 2005). On the other hand, it has been criticized that the interaction of several of these

areas, which are activated during arithmetic fact retrieval, may not be specific to arithmetic fact retrieval. For instance, IFG, STG, and SMG are typically also involved in phonological decoding during language processing (Prado et al., 2011; Vigneau et al., 2006; for a review, see Price, 2012). Similarly, modulation of AG (de)activation, observed for arithmetic fact retrieval, was also found for non-mathematical content (Ischebeck et al., 2007; Zamarian et al., 2009). In a single-case training study, Zaunmueller et al. (2010) examined the fMRI signal in a patient with aphasia, who also showed deficits in multiplication fact retrieval. For untrained problems, the patient demonstrated strong activations in left prefrontal areas and the right posterior AG. This observation corroborates the verbally reported use of back-up strategies, such as the recital of a multiplication row. For trained problems, activation was stronger in a more anterior segment of the right AG, whereby the patient had reported using more retrieval-based strategies. A similar example is provided by a single case reported by Delazer and Benke (1997): After the resection of a left parietal tumor, the patient was no longer capable of understanding arithmetic on a conceptual level, yet was able to produce the correct answer to several arithmetic tasks due to memorised fact knowledge. Therefore, it appears likely that (sub)processes of arithmetic fact retrieval are related to phonological language processing.

However, such an association between arithmetic fact retrieval and language processing is still debated. Amalric and Dehaene (2016, 2017, 2019) suggested that simple, overlearned arithmetic facts might be processed independently of left-hemispheric language areas. Evidence for a dissociation between arithmetic and non-arithmetic fact storage was provided by a case study of semantic dementia (Zamarian et al., 2006). The patient's semantic fact knowledge remained intact, while their non-arithmetic semantic knowledge did not. In particular, the authors proposed that procedure-based calculation and overlearned arithmetic facts are processed within the bilateral fronto-parietal 'math-responsive' network.

However, the empirical evidence concerning this question is still inconsistent on whether arithmetic fact retrieval and language processes recruit overlapping cortical circuits. There seems to be a consensus that arithmetic fact retrieval is processed multi-modularly and distributed in distinct brain regions. Therefore, it is critical to consider network characteristics such as connectivity between distant brain regions and subnetworks.

Studies examining white matter correlates in children point to the importance of fronto-parietal connections in numerical and mathematical cognition (see Matejko & Ansari, 2015; Peters & de Smedt for reviews). For arithmetic fact retrieval in children, Van Beek et al. (2013) found

that fractional anisotropy, a measure of white matter integrity, correlated with multiplication and addition in the left anterior segment of the arcuate fasciculus. Moreover, when controlling for different types of reading measures, this association disappeared. This further corroborates that arithmetic fact retrieval of multiplication relies heavily on phonological processing. Klein et al. (2016) provided further evidence for white matter connectivity underlying arithmetic fact retrieval using probabilistic fiber tracking in healthy adults. The authors showed that parietal areas are connected with frontal areas dorsally via the cingulate bundle and ventrally via the extreme/external capsule system and temporal areas via the inferior longitudinal fascicle. The importance of the integrity of such a network architecture for fact retrieval has already been highlighted in some studies: For instance, in a re-evaluation of a single case reported by Zaunmueller et al. (2009), Klein et al. (2013b) found that the lesion was limited to the basal ganglia region (and did not involve the AG) but nevertheless led to disruption of white matter fibers connecting frontal areas with the AG. Based on this, the authors suggested that the patient could not retrieve arithmetic facts because of disconnection within their retrieval network and not because of actual grey matter damage in cortex areas associated with fact retrieval. In this vein, Mihulowicz et al. (2014) conducted a voxel-based lesion behaviour mapping study (VLBM). VLBM analyses the association of voxel-wise lesion status (lesioned or not lesioned) with a given behavioural variable to map the neural correlates of neuropsychological pathology and the functional anatomy of the human brain (Rorden & Karnath, 2004). For each voxel, the relation between anatomical pathology and behavioural pathology is statistically tested and corrected for multiple comparisons. They observed a significant association of lesions in the dorsal pathway (i.e., parts of the superior lateral fasciculus) with arithmetic fact retrieval.

Only recently, lesion-disconnectome mapping has brought forward the possibility to more closely examine the role of white matter network disruption of brain lesions in post-stroke cognitive deficits. In particular, it allows for an indirect assessment of lesion-induced disconnections by reference to healthy connectome data (e.g., Griffis et al., 2019). Information about a patient's structural lesions is incorporated into a connectome of healthy subjects to estimate potential disconnection. In the current study, we evaluated brain disconnections associated with low performance in arithmetic fact retrieval in acute left- and right-hemisphere stroke patients at the group level. We expected that white matter disconnection of voxels within the left-hemispheric arithmetic fact retrieval network, including, among others, AG and MTG, should be associated with low performance in arithmetic fact retrieval. In a subsequent analysis, we specifically evaluated disconnections between grey matter regions. That is, over the entire

brain, we examined which direct grey matter-to-grey matter disconnections are significantly associated with a low performance in arithmetic fact retrieval. Again, we expect to find that disconnections between grey matter regions involved in the arithmetic fact network are associated with a low behavioural performance. Therefore, the first analysis should provide white matter areas whose level of disconnection is associated with low performance, while the second analysis should provide specific grey matter-to-grey matter disconnections associated with low performance.

2. Methods

2.1 Participants

We used the existing patient data set from Mihulowicz et al. (2014) and added 28 new patients for the present analyses. In total, 73 native German-speaking acute stroke patients participated in the study. All of them were patients consecutively admitted to the Center of Neurology at Tuebingen University Hospital over 33 months (cf. Mihulowicz et al., 2014) plus another 18 months, whereby the experimental tasks and procedure were identical in both data acquisition phases. Among these, 38 patients presented with left hemisphere damage (LHD) and 35 patients with right hemisphere damage (RHD). Patients were only included when they presented an MR- or CT-documented cerebral stroke, not more than 14 days post-onset. We did not include patients with previous lesions, other neurological or psychiatric diseases, or white matter alterations. Patients or their relatives gave their informed consent to participate in the study. The study followed the ethical standards in the Declaration of Helsinki (Version 2013) and was approved by the local ethics committee (Vote 82/2018 BO2). Clinical and demographic data for the whole group of 73 patients are given in Table 1; an illustration of the lesion overlap of all participants can be seen in Figure 1.

Table 1 | Demographic and clinical data of all LHD and RHD patients

	LHD	**RHD**
N	38	35
Sex	19F, 19M	18F, 17M

Age (years)	Mean (SD)	63.05 (14.22)	63.38 (15.37)
Stroke type	Ischemic / Hemorrhage	32 / 6	28 / 9
Interval lesion onset to examination (days)	Mean (SD)	4.8 (2.5)	4.4 (2.3)
Interval lesion onset to imaging (days)	Mean (SD)	2.7 (2.6)	2.7 (3.2)
Education (years)	Mean (SD)	11.27 (4.36)	11.14 (4.43)
Contralateral paresis	% present	52.63	65.71
Visual field deficit	% present	13.16	11.43
Aphasia	% present	42.10	-
Spatial Neglect	% present	-	13.89

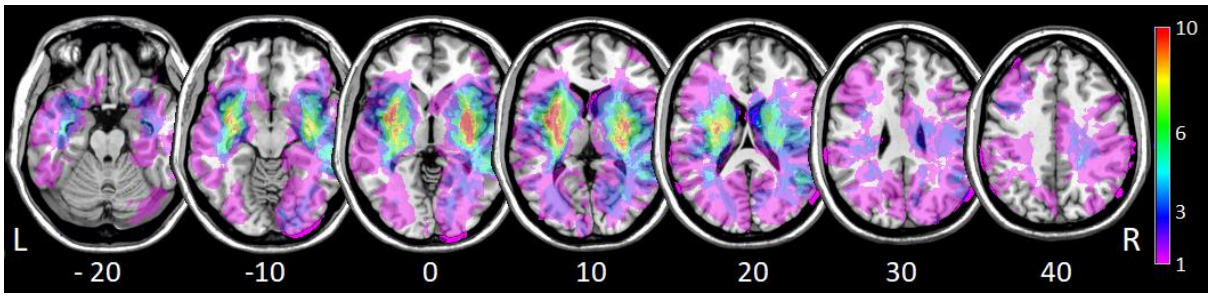

FIGURE 1| Lesion Overlap. Overlap of all lesions included in the analysis. The color bar indicates the frequency of lesion overlap. The vertical z coordinate of standardized MNI space is given below each slice.

2.2 Procedure

Patients were investigated in sitting position. The entire experiment took about one hour and was completed in one session for most patients. For some, further sessions were needed due to clinical examinations or because they needed a break. For the multiplication task, patients responded verbally and in written form when the former was impossible.

We ensured that all patients were able to follow the task instructions. In particular, we tested receptive and expressive language abilities in LHD patients. For *language comprehension*, we used the 'Colour-Figure` subtest from the German adaptation of the Aphasia Check List (ACL; Kalbe et al., 2005). In this task, patients were presented with different coloured shapes. They

were asked to touch them in different syntactical complexities (e.g., “touch the small blue triangle after touching the large blue triangle”). We applied the 'Picture naming task' of the Aachener Aphasia-Bedside Test (AABT; Biniek et al., 1992) to assess language production. Patients were presented with drawings of everyday objects and were asked to name them.

We also tested patients with RHD for *spatial neglect*. The neglect test comprised the 'Letter Cancellation Task' (Weintraub & Mesulam, 1985), the 'Bells test' (Gauthier et al., 1989), as well as a copying task (Johannsen & Karnath, 2004). In the cancellation tasks, patients were presented with arrays of letters and had to cross out ‘A’s (Letter cancellation) or dark objects, such as keys, apples, or bells. Patients had to cross out all bells (Bells cancellation). We calculated the Centre of Cancellation (CoC) for the two cancellation tasks, using the procedure and cut-off scores for diagnosing spatial neglect described by Rorden and Karnath (2010). In the copying task, patients were asked to copy a complex multi-object scene consisting of four figures (a fence, a car, a house, and a tree), with two of them located in each half of the horizontally oriented sheet of paper. The omission of at least one of the contralateral features of each figure was scored as 1. The omission of each whole figure was scored as 2. One additional point was given when contralaterally located figures were drawn on the ipsilesional side of the paper sheet. The maximum score was 8. A score higher than 1 (i.e., > 12.5% omissions) was taken to indicate neglect. Patients were diagnosed with spatial neglect if they scored above the respective cut-off as per the manual in at least 2 out of 3 tests.

Visual field deficits were assessed in all patients via the standard neurological confrontational procedure. Here, the experimenter stands centrally in front of the patient and instructs them to focus on their nose. Then, the experimenter wiggles their finger in the left or right visual field of the patient at different heights. The patient is instructed to report whether the finger moves or not. Table 1 presents all clinical data.

2.3 Stimuli

As part of our battery, we evaluated patients' arithmetic fact retrieval through a single-digit multiplication production task (i.e., 42 items from arithmetical tables up to 9×9), included in the standardized neuropsychological Number Processing and Calculation Battery (NPC; Delazer et al., 2003). Each multiplication problem was presented on a separate A4 sheet (black digits printed on white paper, digit height: 7 mm). Sheets were aligned centrally on a table in front of the patient. According to the standardized NPC procedure, testing was stopped after

five consecutive incorrect or missing responses, and no time limit was imposed. However, responses lasting longer than 10 seconds were rated as incorrect, as this implies a failure in instant fact retrieval. Self-corrections were allowed. In addition and subtraction, 67 out of 73 patients made a maximum of two errors, which is non-pathological (see supplementary table S1). This lack of behavioural variance made lesion analysis unviable specifically for addition and subtraction.

One aphasic LHD patient could not solve the single-digit multiplication production task orally or in writing, while he could solve 24 of 25 addition tasks correctly in verbal form (over the cutoff time of 10 seconds). In this patient, we applied a multiple-choice version of the multiplication task also provided in the NPC to determine a core deficit in multiplication processing rather than a language difficulty. The multiple-choice version tested the same multiplication problems (e.g., 6 x 7) but provided four solution probes (i.e., correct solution, 42; one operand error, e.g., 45, one table error, e.g., 49, and one close-miss error, e.g., 39). The patient showed deficits in the multiple-choice version. Accordingly, his score of 0 in the multiplication production task was included in the data analysis.

2.4 Lesion Analysis

We used diffusion-weighted MRI images taken within 48h after stroke (Weber et al., 2000) or else T2-weighted fluid-attenuated inverse-recovery (FLAIR) images (Brant-Zawadzki et al., 1996; Noguchi et al., 1997; Ricci et al., 1999; Schaefer et al., 2002). In case MR imaging was not conducted, CT images were used (MRI: *N*=29; CT: *N*=44). When several imaging data sets existed for an individual patient, we used the session closest in time to behavioral testing showing a clear demarcation. Lesion borders were marked semi-automatically using the 'Clusterize Toolbox' (de Haan et al., 2015). Then, both the anatomical scan and the lesion map were normalized into stereotaxic space using the 'Clinical Toolbox' (Rorden et al., 2012; www.mccauslandcenter.sc.edu/CRNL/clinical-toolbox) implemented in SPM12 (www.fil.ion.ucl.ac.uk/spm).

2.5 Whole-brain disconnectivity mapping

We created individual white matter disconnectivity topographies for each patient. These topographies indicate the proportion of disconnected fibers for each white matter voxel in the

brain imaging space running through this voxel. Thereby, it allows a topographical assessment of a lesion's impact on brain connectivity as a whole. To this end, we applied the Lesion Quantification Toolkit (LQT; Griffis et al., 2021). The LQT utilizes a tract-wise connectome atlas and embeds the patient's lesion map into it. The toolkit identifies all fiber streamlines that intersect with the lesion and maps connectome-wide disconnection induced by the lesion. In other words, each voxel value corresponds to the percentage of all streamlines within this voxel that are expected to be disconnected by the lesion. We used the LQT's standard HCP-842 atlas (Yeh et al., 2018) for atlas-based tractography, keeping the default parameter setting as suggested in the LQT manual.

Subsequently, we further analyzed these continuous disconnectivity maps using mass-univariate General Linear Models in 'NiiStat' (https://github.com/neurolabusc/NiiStat). In this analysis, the predictor variable was the previously mentioned percentage value of disconnected streamlines of a voxel, while the outcome variable was the multiplication score. Only voxels with a disconnection in at least five patients were considered in the analysis. Tests were performed one-sided at $p<0.05$ and corrected for family-wise errors. The family-wise error rate was corrected using 5000 permutations with maximum statistic permutation (Nichols & Holmes, 2002). This disconnectivity topography mapping thus identified voxels for which disconnection is associated with low performance in multiplication. As the patient with a multiplication score of 0 may have affected the results disproportionally, we reran the analyses excluding this patient.

2.6 Whole-brain Bayesian disconnectivity mapping

Using the aforementioned disconnection maps, we used custom code written in R (R Core Team, 2022) to correlate the voxel-wise percentage of disconnected streamlines with the multiplication score and to derive a Bayes Factor for each voxel. The Bayes factor describes the relative difference in evidence for H1 compared to H0. Thus, it enables the quantification of evidence for or even against an effect independently of an arbitrary cut-off such as the p-value, transparently highlighting limitations in statistical power when evidence for neither hypothesis is strong. Again, only voxels with a disconnection in at least five patients were considered. This second disconnectivity topography thus quantified the evidence for each voxel disconnection's association with low performance in multiplication. As above, we ran the analysis twice: Once including and once excluding the patient with 0 points in the multiplication task.

2.7 Region-to-region disconnectivity

We additionally analyzed parcel-wise disconnectivity as provided by the LQT. This procedure allowed us to identify which direct disconnections between two grey matter regions are significantly associated with low performance in the multiplication task. We created a structural connectivity matrix by combining the provided tractography atlas and the Brainnetome Atlas (BN-246, Fan et al., 2016) as our grey matter parcellation atlas. The BN-246 is multi-modally derived, contains 210 cortical and 36 subcortical subregions, and was developed specifically for connectivity analyses. The number of streamlines disconnected by the lesion map between each pair of parcels was converted to a percentage of disconnected streamlines, resulting in symmetric 246-by-246 disconnectivity matrices. Each value in this matrix denotes the percentage of disconnected streamlines between two given grey matter areas. We subjected these matrices to a mass-univariate analysis to identify associations between disconnection and low performance in multiplication using custom scripting in MATLAB R2020a. Following the strategy of the topographical analysis of brain-wide disconnectivity maps described above, we employed mass-univariate general linear models with a family-wise error correction by maximum statistic permutation (Nichols & Holmes, 2002).

We loaded disconnection matrices into MATLAB and removed the diagonal and redundant elements below it. Many ROI-to-ROI disconnections were rarely or never present in the data, likely either because the sample's lesion anatomy did not include damage to the connection or because the connection was physiologically non-existent. Therefore, we identified the sum of all patients with a disconnection present (i.e., a disconnection score > 0) for each ROI-to-ROI connection. We removed all connections affected in less than 15 patients from the analysis, reducing the final set of analyzed connections to 955 (see Sperber et al., 2022). We then computed a general linear model for each ROI-to-ROI connection with the independent variable disconnectivity score and the dependent variable multiplication performance. Then, maximum statistic permutation with 50.000 permutations was employed on permuted behavioral data and the original disconnection data with the same analysis strategy to assess the distribution of maximum statistics under the null hypothesis. We obtained a one-sided, corrected threshold for statistical significance at $p < 0.05$ by identifying the 95^{th} percentile of permutation-derived maximum statistics. As above, the patient with a multiplication score of 0 may have affected the results disproportionally. Therefore, we also analysed the data excluding this patient.

295
296
297 2.8 Region-to-Region disconnectivity using Bayesian hypothesis testing
298 To quantify the evidence for the association of disconnections with multiplication performance
299 (see Keysers et al., 2020), we used the identical method as in the previous section, except that
300 we used a correlation with Bayesian hypothesis testing instead of a frequentist GLM with
301 permutation correction. We used the approach and code provided by Wetzels and
302 Wagenmakers (2012). This analysis enables the continuous quantification of evidence for or
303 against an association of disconnection with multiplication performance. We also analysed the
304 data excluding the patient with 0 points.

305 2.9 Data availability statement
306 Online materials, including all analysis scripts, descriptive data, and resulting topographies, are
307 publicly available at http://dx.doi.org/10.17632/yjkr647mzb.1. The clinical datasets analyzed
308 in the current study are not publicly available due to the data protection agreement approved
309 by the local ethics committee and signed by the participants.
310

311 # 3. Results

312 ## 3.1 Behavioral measures

313 Table 2 summarizes the behavioral results of the multiplication task. Items involving '0' or '1'
314 as operands (n=6) were excluded from the analysis because they address rule-based processing
315 (McCloskey et al., 1991). While the analysis used continuous values, five patients in the RHD
316 group performed below the typical cut-off in the multiplication task; in the LHD group, ten
317 patients did so, including one aphasic patient who could not respond to the multiplication task
318 orally or in writing. As that patient also showed deficits in the aforementioned multiple-choice
319 task but could carry out some other tasks, they were included in the analysis with 0 points for
320 the current task.
321

Table 2 | Raw scores (number of items solved correctly) observed for the two patient groups in the multiplication task

	LHD (n = 38)	RHD (n = 35)

	Items	Mean	Median	SD	Range	Mean	Median	SD	Range
Multiplication	36	29.73	33	8.91	0-36	32.92	34	4.14	21-36

3.2 Brain-wide disconnectivity mapping

Figure 2 (Panel A) illustrates the average percentage of lesion-induced disconnection for all 73 patients. Low single-digit multiplication performance was significantly associated with the disconnection of a single cluster around x = (-59; -40), y = (-57; -39), and z = (3; 22), affecting areas defined by the HCP-842 as the left arcuate fasciculus, temporo-pontine tract, and U-fibers between the AG and superior temporal areas (see Figure 2, Panel B).

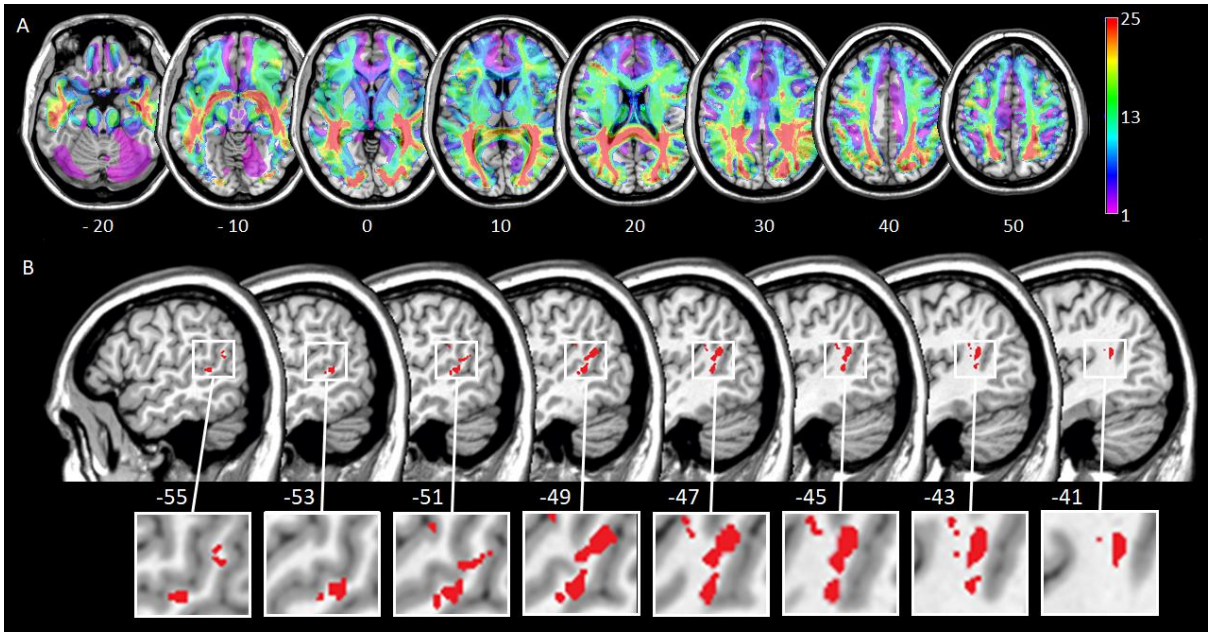

FIGURE 2 | Frequentist disconnectivity mapping. (A) The percentage of fiber disconnection, as indicated by the average reduction in streamline density, is color-coded from 1 (pink) to 25 (red), whereby the maximum value in a voxel was 36. A higher number indicates a higher percentage of fiber disconnection. Topographies can be viewed in the online data. The vertical z coordinate of standardized MNI space is given below each slice. (B) Sagittal view of the left hemisphere. Statistical voxel-wise lesion-behavior mapping (VLBM) analyses using mass-univariate general linear models in multiplication. Plotted are voxels that survived permutation-based FWE correction at $p < 0.05$. The sagittal x coordinate of standardized MNI space is given below each slice.

As one patient had a multiplication score of 0, their response may have influenced the results disproportionally. When this patient was excluded from the analysis, no voxels reached significance. To quantify the evidence of an effect in those voxels independently of a significance threshold, we also carried out the same analysis using Bayesian null hypothesis testing (BNHT) once with, and once without the outlying patient.

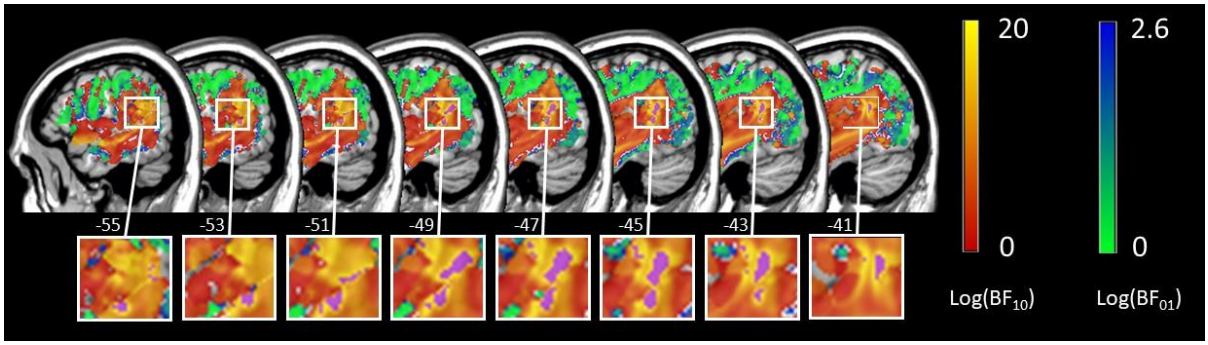

FIGURE 3 | Bayesian disconnectivity mapping. Sagittal view of the left hemisphere. The heatmap denotes log-Bayes factors of correlations between voxel-wise disconnection value and multiplication score, as some values were so large that MRIcron could not display them. Voxels marked in a red-to-yellow manner had BFs indicating evidence for their association with multiplication score, while voxels marked in green-to-blue indicate evidence for no association with multiplication score. Purple indicates the voxels that were significant following the frequentist analysis (see Figure 2). The sagittal x-coordinate of standardized MNI space is given below each slice. Note that log(1) = 0, therefore if a voxel has value 0, the BF for this voxel = 1 (i.e., when the evidence for H1 and H0 are equal).

Figure 3 shows the results of the brain-wide disconnectivity mapping using BNHT while including all patients. The largest BFs were found in nearly the identical voxels as in the frequentist analysis, in a cluster around the left AG (see panel B). Additionally, the continuous mapping of BFs also uncovered a cluster ranging from the AG down to anterior segments of the STG. When excluding the patient with zero points, the general pattern of results remained the same, only that BFs were smaller (see Appendix A).

3.3 Region-to-region disconnectivity

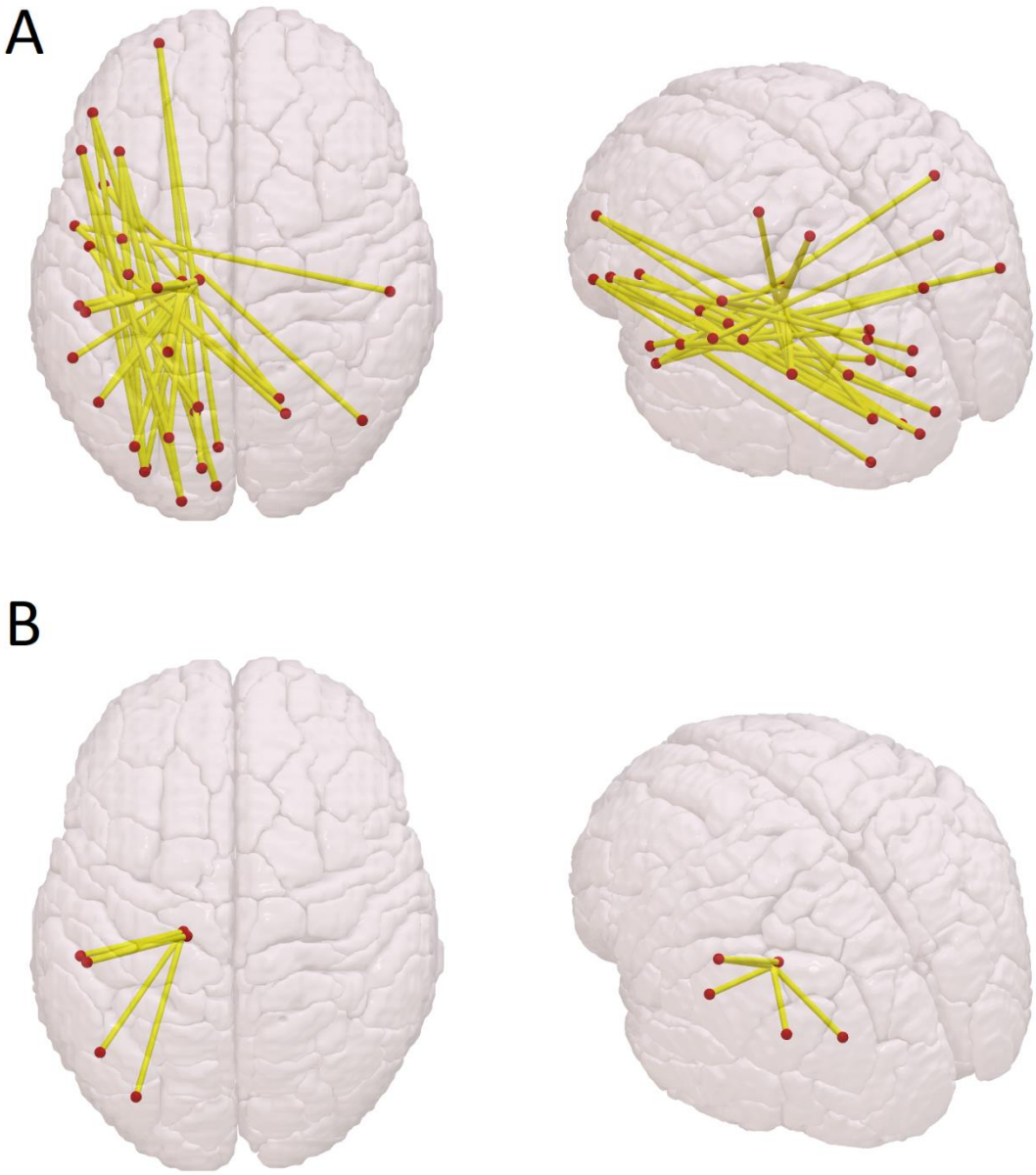

Figure 5 | Parcel-to-parcel disconnections following the region-to-region disconnectivity analysis. The image presents the disconnections significantly associated with a low multiplication performance following the permutation-based GLM (A) with all patients and (B) when excluding the patient with zero points.

Mapping multiplication score to ROI-to-ROI disconnectivity using general linear models identified 41 connections significant at $p < 0.05$ (see Figure 5 (Panel A), Table 3). The disconnectome revealed several regions that stood out due to several disconnections associated with low performance in multiplication. A hub-like structure was found for the left thalamus, with 18 disconnections mainly to the left inferior and superior parietal lobules, including PGa of the angular gyrus. Furthermore, 14 disconnections between the left IFG and the medioventral occipital cortex as well as the left lateral occipital cortex were also associated significantly with

poorer multiplication scores. Finally, further 5 disconnections from the left STG to the right inferior and superior parietal lobules (IPL, SPL), as well as to the right precuneus, were significant. When excluding the patient with zero points in the multiplication task, only 5 disconnections were left over. Four were from the left sensory thalamus to areas PGp, PFt, PGa, PFop of the left IPL and one was from the left posterior parietal thalamus to the left PFt (Figure 5, Panel B).

Side	Lobe	Gyrus	Name	Name	Gyrus	Lobe	Side
Left	F	IFG	A44op, opercular area 44	OPC, occipital polar cortex	LOccC	O	Left
			A44op, opercular area 44	iOccG, inferior occipital gyrus			Left
			A44op, opercular area 44	msOccG, medial superior occipital gyrus			Left
			A44op, opercular area 44	lsOccG, lateral superior occipital gyrus			Left
			A44op, opercular area 44	mOccG, middle occipital gyrus			Left
			A45c, caudal area 45	OPC, occipital polar cortex			Left
			A45c, caudal area 45	msOccG, medial superior occipital gyrus			Left
			A45c, caudal area 45	lsOccG, lateral superior occipital gyrus			Left
			A45c, caudal area 45	mOccG, middle occipital gyrus			Left
			A45r, rostral area 45	iOccG, inferior occipital gyrus			Left
			A44op, opercular area 44	cCunG, caudal cuneus gyrus	MvOccC		Left
			A44op, opercular area 44	cLinG, caudal lingual gyrus			Left
			A45r, rostral area 45	cCunG, caudal cuneus gyrus			Left
			A45r, rostral area 45	cLinG, caudal lingual gyrus			Left
		MFG	A10l, lateral area10	cLinG, caudal lingual gyrus			Left
			A10l, lateral area10	rCunG, rostral cuneus gyrus			Left
		PrcG	A4ul, area 4upper limb region	PPtha, posterior parietal Thal	Thal	S	Left
			A4ul, area 4upper limb region	lPFtha, lateral pre-frontal Thal			Left
	I	IG	dla, dorsal agranular insula	OPC, occipital polar cortex	LOccC	O	Left
			dla, dorsal agranular insula	mOccG, middle occipital gyrus			Left
			G, hypergranular insula	dlg, dorsal granular gyrus	IG	I	Left
	O	LOccC	lsOccG, lateral superior occipital gyrus	PPtha, posterior parietal Thal	Thal	S	Left
			mOccG, middle occipital gyrus	PPtha, posterior parietal Thal			Left
			msOccG, medial superior occipital gyrus	Stha, sensory Thal			Left
		MvOccC	rCunG, rostral cuneus gyrus	NAC, nucleus accumbens	BG	S	Left
	P	IPL	A39c, caudal area 39PGp	dlPu, dorsolateral putamen			Left
			A39c, caudal area 39PGp	Stha, sensory Thal	Thal		Left
			A39c, caudal area 39PGp	PPtha, posterior parietal Thal			Left
			A39rd, rostrodorsal area 39 Hip3	PPtha, posterior parietal Thal			Left
			A39rd, rostrodorsal area 39 Hip3	Otha, occipital Thal			Left
			A39rd, rostrodorsal area 39 Hip3	cTtha, caudal temporal Thal			Left
			A39rd, rostrodorsal area 39 Hip3	lPFtha, lateral pre-frontal Thal			Left
			A39rv, rostroventral area 39PGa	Stha, sensory Thal			Left
			A39rv, rostroventral area 39PGa	PPtha, posterior parietal Thal			Left
			A39rv, rostroventral area 39PGa	cTtha, caudal temporal Thal			Left
			A40c, caudal area 40PFm	Stha, sensory Thal			Left
			A40c, caudal area 40PFm	PPtha, posterior parietal Thal			Left
			A40c, caudal area 40PFm	lPFtha, lateral pre-frontal Thal			Left
			A40rd, rostrodorsal area 40 PFt	Stha, sensory Thal			Left
			A40rd, rostrodorsal area 40 PFt	PPtha, posterior parietal Thal			Left
			A40rd, rostrodorsal area 40 PFt	cTtha, caudal temporal Thal			Left

		A40rd, rostrodorsal area 40 PFt	lPFtha, lateral pre-frontal Thal			Left
		A40rv, rostroventral area 40PFop	Stha, sensory Thal			Left
		A40rv, rostroventral area 40PFop	PPtha, posterior parietal Thal			Left
	PocG	A1/2/3ulhf, area 1/2/3upper limb, head and face region	lPFtha, lateral pre-frontal Thal			Left
	Prec	dmPOS, dorsomedial parietooccipital sulcusPEr	PPtha, posterior parietal Thal			Left
	SPL	A7pc, postcentral area 7	Stha, sensory Thal			Left
		A7c, caudal area 7	PPtha, posterior parietal Thal			Left
		A7pc, postcentral area 7	PPtha, posterior parietal Thal			Left
		A7ip, intraparietal area 7hIP3	PPtha, posterior parietal Thal			Left
T	STG	A22r, rostral area 22	A40rv, rostroventral area 40 PFop	IPL	P	Right
		A38l, lateral area 38	A39c, caudal area 39PGp			Right
		A38l, lateral area 38	A39rd, rostrodorsal area 39 Hip3			Right
		A22r, rostral area 22	dmPOS, dorsomedial parietooccipital sulcus, PEr	Prec		Right
		A38l, lateral area 38	dmPOS, dorsomedial parietooccipital sulcus, PEr			Right
		TE1.0 & TE1.2	dmPOS, dorsomedial parietooccipital sulcusPEr			Left
		A22r, rostral area 22	A7c, caudal area 7	SPL		Right
		A38l, lateral area 38	A7c, caudal area 7			Right
		A38l, lateral area 38	V5/MT+	LOccC	O	Right
		A38l, lateral area 38	lsOccG, lateral superior occipital gyrus			Right
		TE1.0 & TE1.2	msOccG, medial superior occipital gyrus			Left
		TE1.0 & TE1.2	lsOccG, lateral superior occipital gyrus			Left
		A22r, rostral area 22	rCunG, rostral cuneus gyrus	MvOccC		Right
		TE1.0 & TE1.2	vmPOS, ventromedial parietooccipital sulcus			Left
S	BG	dlPu, dorsolateral putamen	A7m, medial area7 PEp	Prec	P	Right
		NAC, nucleus accumbens	A7m, medial area7 PEp			
		NAC, nucleus accumbens	dmPOS, dorsomedial parietooccipital sulcusPEr			
		NAC, nucleus accumbens	A31, area 31 Lc1			

Table 3 | Parcel-to-parcel disconnections significantly associated with a low multiplication performance following the region-to-region disconnectivity analysis at $p < .05$ (corresponding to Figure 3A). Each row denotes the side, lobe, gyrus and exact lable according to the BN-246 (Fan et al., 2016) of each grey matter-to-grey matter disconnection. F = frontal, I = Insular, O = Occipital, P = Parietal, T = Temporal, S = subcortical, IFG = Inferior Frontal Gyrus, MFG = Middle Frontal Gyrus, PrcG = Precentral Gyrus, IG = Insular Gyrus, LOccC = Lateral Occipital Cortex, MvOccC = Medioventral Occipital Cortex, IPL = Inferior Parietal Lobule, PocG = Postcentral Gyrus, Prec = Precuneus, SPL = Superior Parietal Lobule, STG = Superior Temporal Gyrus, BG = Basal Ganglia, Thal = Thalamus

3.4 Bayesian Region-to-region disconnectivity

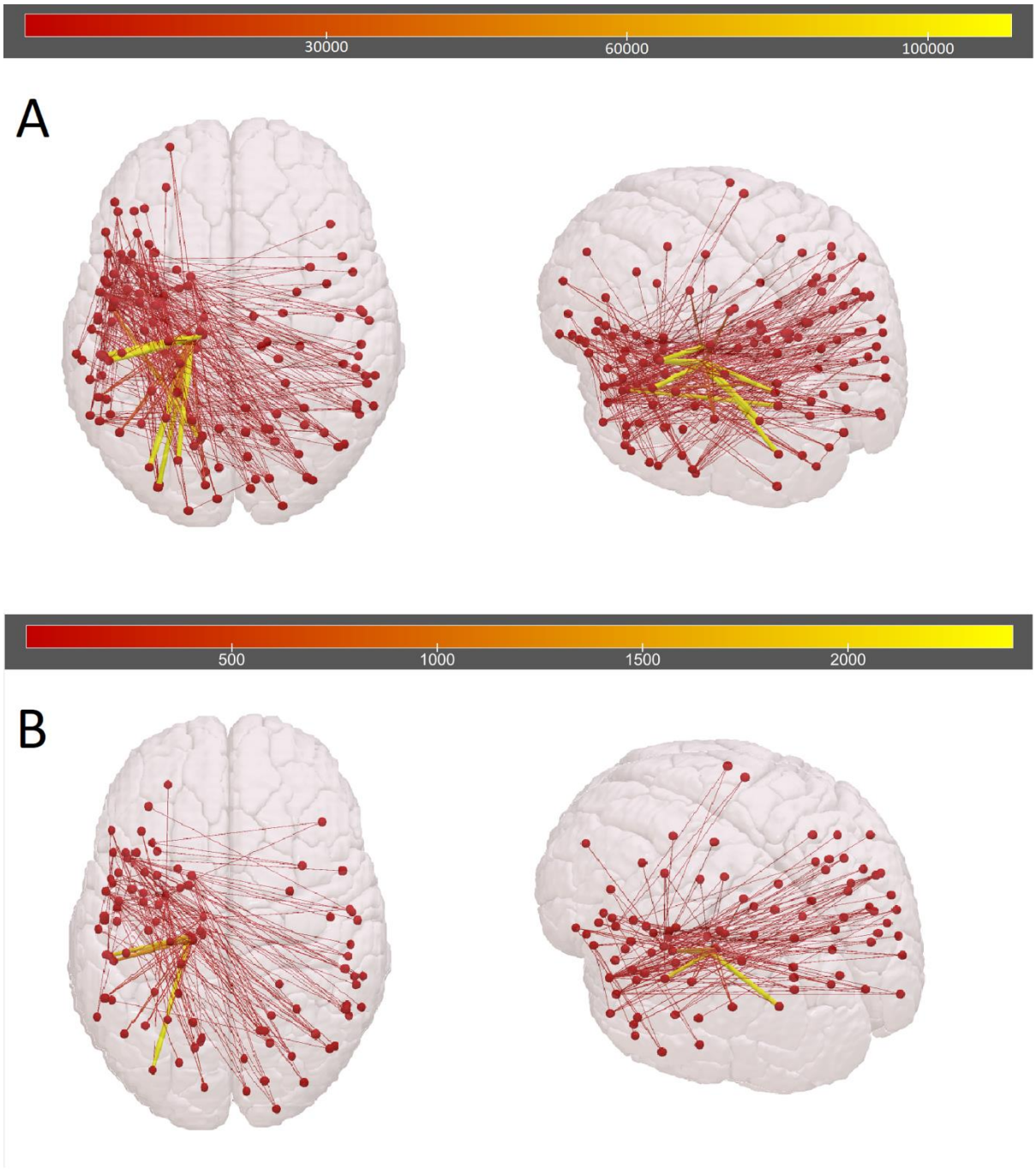

Figure 6 | Parcel-to-parcel disconnections following the Bayesian region-to-region disconnectivity analysis. The images presents the disconnections associated with a low multiplication performance following BNHT with a BF > 3 (A) with all patients and (B) when excluding the patient with zero points. Color scales reflect BF values whereby thicker and more yellow edges denote higher BF.

Mapping multiplication score to ROI-to-ROI disconnectivity using Bayesian hypothesis testing identified 313 connections with a $BF_{10} > 3$ suggesting evidence for H1, an effect of disconnection on multiplication performance (see Figure 6, Panel A). Of the 7 disconnections with the largest BFs ($BF_{10} > 10^5$), 6 were from the left thalamus to the left IPL, and one from the left thalamus to the left middle occipital gyrus (yellow bars in Figure 6, Panel A). A table including all values for all comparisons can be found in the supplementary material.

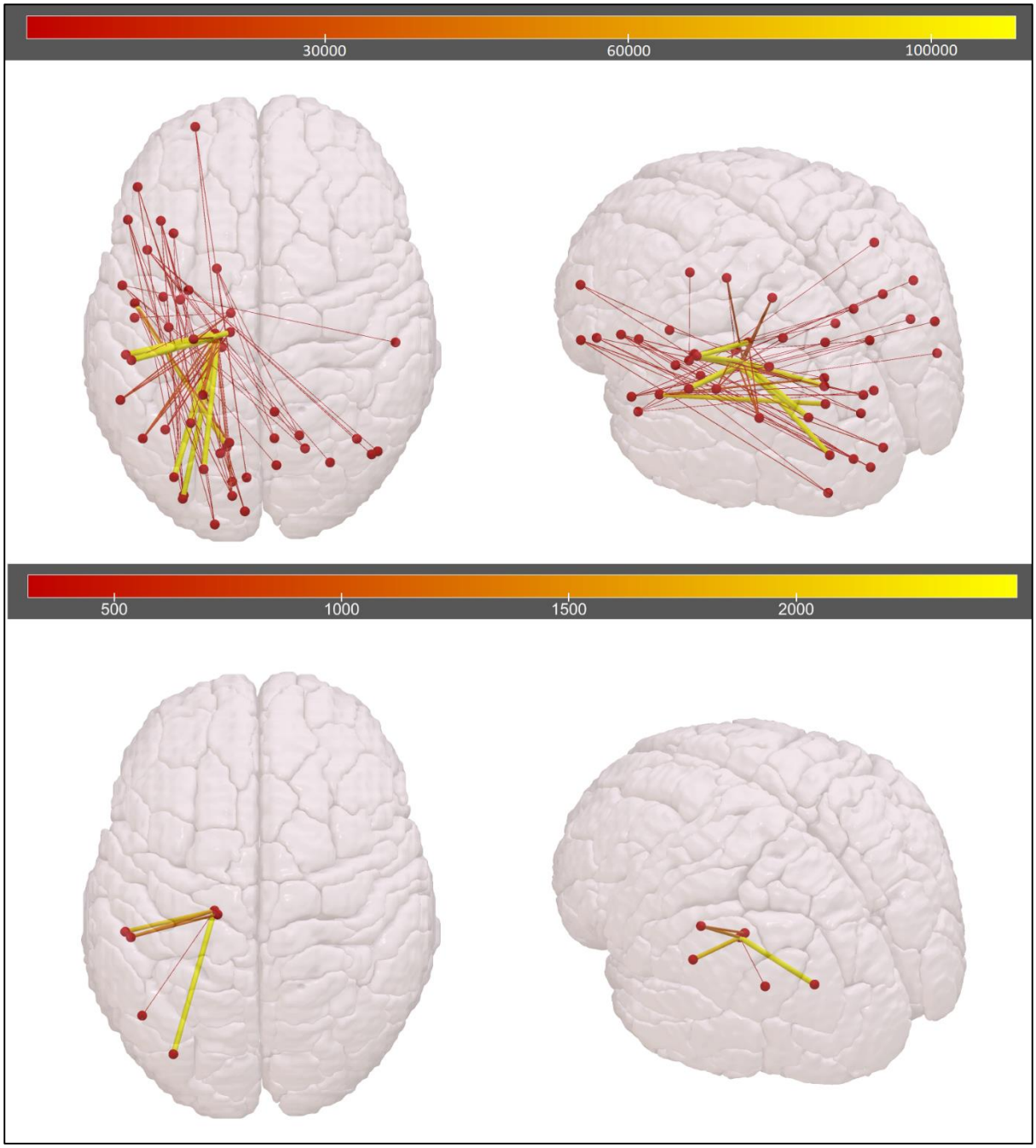

Figure 7 | Parcel-to-parcel disconnections following the Bayesian region-to-region disconnectivity analysis. The images present the disconnections associated with a low multiplication performance following BNHT with a BF > 311, making them comparable to those derived from the permutation-based approach, as they are nearly equal to those that were significant in the frequentist analysis (A) with all patients and (B) when excluding the patient with zero points. Color scales reflect BF values whereby thicker and more yellow edges denote higher BF.

In Figure 7, Panel A, only disconnections with a $BF_{10} > 311$ are presented, to show that this analysis is comparable to the permutation-based approach. These values suggest extreme evidence for an effect (see Lee & Wagenmakers, 2013). This pattern looks identical to the results provided by the GLM analysis. Again, hub-like structures were found for the left thalamus, with 22 disconnections mainly to the left inferior and superior parietal lobules, 3 to the left occipital gyrus, and 2 to the left precentral gyrus; the left IFG with 14 disconnections to the left medioventral occipital cortex as well as the left lateral occipital cortex; and the left STG, with 13 disconnections to the right inferior and superior parietal lobules (IPL, SPL), the left and right precuneus, and right occipital areas. The disconnections with the strongest evidence (BF > 50,000) were from the left parietal lobe to the thalamus, the left occipital lobe to the thalamus, and one from the left occipital lobe to the left temporal lobe.

Similarly, when excluding the patient with 0 points, the same pattern of disconnections was observed at a $BF_{10} > 311$ as in the permutation-based GLM (compare Figure 5B and 7B).

All in all, when comparing the results of the permutation-based analysis and the BNHT analysis with or without the patient scoring zero points in the multiplication task, the most robust disconnections appear to be those between the left IPL to the left thalamus.

4. Discussion

The present study evaluated how white matter disconnection affected arithmetic fact retrieval. With the present patient sample it was not possible to examine the role of damage to grey matter, as most lesions of our patients were within white matter (see lesion overlap, Figure 1), providing insufficient power to analyse voxels within grey matter (see Kimberg et al.,2007). We carried out four lesion-disconnection analyses in first-time stroke patients with unilateral damage to either the left or right hemisphere performing a multiplication task. In the first analysis, patients' lesions were superimposed on a white matter tractography map, leading to

individual disconnection topographies (Griffis et al., 2019). A whole-brain univariate analysis suggested that disconnection of white matter fibers situated between the anterior AG and posterior STS was associated with poorer multiplication performance. A second analysis was carried out to investigate direct disconnections between two brain areas that could lead to low multiplication performance. Single brain areas were defined as ROIs by a connectivity-based grey matter atlas, and disconnection between each pair of regions was investigated for its role in multiplication performance. We found several structures with multiple relevant disconnections. These included the left thalamus, the left IFG, left and right (intra)parietal areas such as the AG, STG, and left occipital areas. Single disconnections with the strongest disconnection-deficit association were found between the left thalamus and the left IPS as well as left occipital regions, but also between the left primary auditory cortex and left occipital areas. As the patient with 0 points in the multiplication task affected some disconnections disproportionally, we also replicated the previous analyses using Bayesian hypothesis testing to quantify the evidence for the effect of disconnections on multiplication score, once with and once without said patient. The most influential disconnections (i.e., those with the highest Bayes Factors) when including all patients were almost identical to those in the previous analysis using frequentist testing. Bayes Factors decreased when excluding the patient with 0 points, but the disconnection pattern was almost the same. The strongest disconnections were from the left IPL to the left thalamus, followed by disconnections of the left IFG to left occipital areas, again followed by several disconnections of the left STG and MTG to the right IPL. The results of these analyses will be discussed in turn in the following.

Whole-Brain Analysis: Disconnection of the left AG with temporal areas

The findings of the whole-brain analysis fit well with a connectivity model of arithmetic fact retrieval put forward by Klein et al. (2016). In this model, connections between the left MTG and the left AG were considered necessary for arithmetic fact retrieval, as both areas are essential elements of a left-hemispheric arithmetic fact retrieval network. A significant role of the left AG for arithmetic fact retrieval has also been suggested by several neuropsychological single case studies on arithmetic fact retrieval (e.g., Hittmair-Delazer et al., 1994; Lee, 2000; Cohen et al., 2000). However, other single case studies have questioned the importance of the AG within this network, as they reported patients presenting with a multiplication deficit despite having a preserved AG (Cohen et al., 2000; Dehaene & Cohen, 1997; van Harskamp et al., 2005; Zaunmueller et al., 2009). For example, patient ATH had severe difficulties verbally solving multiplication problems while making only a few mistakes in subtraction (Cohen et al.,

2000). On the other hand, Van Harskamp & Cipolotti (2001) reported on a patient who did not show a multiplication deficit, although damage to left parietal regions, including the AG, occurred.

Given both the current results and more recent research, inconsistent results of single case studies can be explained by the approach of Klein and colleagues (2016): The disconnection cluster indicated by our analysis to be associated with arithmetic fact retrieval involved the left arcuate fasciculus, the temporopontine tract and U-fibers between the AG and STS. This observation suggests that disconnection of the AG with temporal areas, such as STS, STG, and MTG seems to cause an arithmetic fact retrieval deficit. This expands the results of previous studies indicating the detrimental effect of lesions to or disconnection of the AG. In this sense, Klein et al. (2013b) re-evaluated a single case reported by Zaunmueller et al. (2009), focusing on lesions to the patient's white matter compared to previous single case studies focusing on lesions more on grey matter damage. While the lesion itself was in the basal ganglia, it also incorporated white matter fibers that explicitly connect frontal areas with the AG, suggesting that the patient could not retrieve arithmetic facts due to poor connectivity of the AG. Similarly, Mihulowicz et al. (2014) conducted a voxel-based lesion behavior mapping study observing that white matter lesions to superior parts of the superior lateral fasciculus (SLF II) impaired arithmetic fact retrieval.

The current findings provide the first evidence of indirect measures of disconnection on arithmetic fact retrieval on the group level, further corroborating the role of the left AG within the arithmetic fact retrieval network. They can explain case studies questioning the role of the left AG in multiplication, whereby patients with multiplication deficits without damage to the AG or other grey matter areas of the network may have suffered from structural white matter disconnectivity within the network, as suggested by Klein et al. (2013b, c).

Importantly, neurofunctional evidence from healthy participants on learning complex multiplication facts (e.g., Delazer et al., 2003, 2005; Ischebeck et al., 2006, 2007; Grabner et al., 2009; Rickard et al., 2000; Zamarian et al., 2009) also indicates that the left AG plays a crucial role in arithmetic fact retrieval. Bloechle et al. (2016) evaluated fMRI signal before and after multiplication training. They found a stronger fMRI signal in the left AG when comparing trained vs. untrained multiplication tasks after training only, but no difference in activation when directly comparing the same multiplication problems across training (post- vs. pre-training). Therefore, the authors suggested that the left AG might act as a 'circuit breaker',

coordinating whether a task is to be solved purely via fact retrieval or whether a switch in strategy requiring additional cognitive processing, such as calculation, is necessary.

This aspect provides a compelling explanation for patient FS's ability to multiply correctly despite damage to parietal areas, including the left AG: They were still able to recall multiplication facts due to an intact temporal retrieval network and did not require the left AG to switch from fact retrieval to calculation. In the current study, most patients with an arithmetic fact retrieval deficit also suffered from aphasia. Accordingly, they might not have been able to recall phonologically stored arithmetic facts initially. When attempting to switch to a calculation-based strategy, these patients were also slowed due to the disconnection of left AG. Therefore, a possible explanation for the given findings may be that when arithmetic fact retrieval fails, the AG is involved in switching the strategy by which a task is solved. When it is disconnected or damaged, this switch fails.

Region-to-Region Disconnectivity

Results of the region-to-region disconnectivity analyses indicate several disconnections between left-hemispheric areas, as well as from left temporal areas to right parietal areas, being associated with deficits in arithmetic fact retrieval. Several disconnection groupings were significant (Fig. 3). First off, all analyses found the most disconnections of the left thalamus with parietal areas (see also Fig. 7), meaning that these results were robust over both the permutation approach as well as BNHT, with and without the patient with zero points in the task. This suggests that a disconnection of the left thalamus with left parietal areas was most likely to lead to a low multiplication performance in the current sample. This fits with previous evidence that both areas are involved in arithmetic fact retrieval (e.g., Arsalidou & Taylor, 2011). In particular, the thalamus is generally involved in various cognitive processes, such as memory, language or mental set-shifting (see Saalmann & Kastner; 2015 for an overview). Therefore, it seems sensible that it also is involved in mental arithmetic (Arsalidou & Taylor, 2011; Johnson & Ojemann, 2000; Koyama et al., 2020). On the other hand, the IPS is known to be involved specifically in magnitude processing (for meta-analyses, see Arsalidou & Taylor, 2011; Arsalidou et al., 2018; Dehaene et al., 2003; Hawes et al., 2019).. Yet, arithmetic tasks are typically not solved exclusively by either arithmetic fact retrieval or magnitude manipulations (i.e., calculations). Instead, they are solved by an adaptive interplay between both (Klein et al., 2016). It thus seems possible that arithmetic fact retrieval deficits following disconnection between the thalamus and the IPS reflect difficulties in switching between and

integrating fact retrieval and magnitude manipulation strategies, as already argued on the whole-brain level. In conclusion, the thalamus may be considered as a sort of central relay of information between different cortical areas, receiving, coordinating, and transmitting information across the cortex. Therefore, it should not be surprising that disconnection of such a vital structure with areas associated with number processing, such as left-hemispheric parietal areas, would lead to deficits in multiplication.

Our results also showed several disconnections of the left IFG with left (parieto-)occipital areas. While previous research reported essential connections between parietal regions, such as the AG, and the IFG (e.g., Klein et al., 2016), the role of fronto-occipital connections in arithmetic has not been focused on so far. However, it is known that the IFG is connected with the parietal and occipital cortex via the inferior fronto-occipital fasciculus (IFOF). This suggests that disconnection of certain parts of the IFOF may also lead to arithmetic fact retrieval deficits. The EC/EmC system corresponds to a rostral/anterior segment of the IFOF (Willmes et al., 2014) and is considered as part of a ventral pathway involved in arithmetic fact retrieval (Klein et al., 2016). More precisely, Klein et al. (2013b) found that arithmetic tasks that can be solved via arithmetic fact retrieval were associated with a ventral processing route. This route ranges from frontal regions, such as the medial frontal gyrus, to parietal regions, including the AG via the middle longitudinal fascicle (MdLF), which itself is part of the EC/EmC system. They suggested that this connection serves the purpose of phonological or semantic access, similar to language processes (e.g., Saur et al., 2008; Weiller et al., 2011). Therefore, in the current study, the observed disconnections might have led to language-related errors, such as semantic or phonemic paraphasias.

Finally, we observed several disconnections of the left STG associated with an arithmetic fact retrieval deficit. Most of these disconnections were to areas around the IPS bilaterally. Disconnections of the left STG to left IPS fit well with a series of fMRI studies in healthy adults (Prado et al., 2011) as well as children with and without mathematical learning disabilities (e.g., Berteletti et al., 2011; Demir et al., 2014) that suggest that the STG, as well as the MTG, play a role in arithmetic fact retrieval. Regarding the results on disconnections to the right IPS, it has been shown several times by Semenza and colleagues that the right parietal cortex is crucially involved in multiplication tasks: For example, Semenza et al. (2017) applied direct cortical stimulation to patients during tumor resection. These were carrying out a multiplication task while having either their left or their right parietal cortex stimulated. When the right parietal cortex was stimulated, patients tended to make more retrieval-based errors

(i.e., deriving wrong solutions within multiplication tables) compared to approximation errors (a number numerically close to the correct solution). In contrast, when their left parietal cortex was stimulated, this proportion changed to about half retrieval-based, and half approximation-based errors. In two further studies examining multiplication with MEG (Arcara et al., 2021; Salillas et al., 2021), the role of right parietal and frontal areas was substantiated, adding to existing evidence. This suggests that the right parietal cortex plays an important role in examining the 'plausibility' of a solution generated by the left hemisphere by estimating the approximate magnitude of the solution. Therefore, it is possible that in case a patient retrieved a wrong solution, the disconnection of right parietal areas may have impaired this estimation of approximate magnitude and thus a reappraisal of the initially retrieved response.

The bilateral arithmetic fact retrieval network

Taken together, the current results indicate that arithmetic fact retrieval in multiplication is subserved by a widely connected network including the left-hemisphere areas suggested by Klein et al. (2016) as well as areas around the right IPS. The whole-brain analyses corroborated the idea that the left angular gyrus plays a central role in arithmetic fact retrieval (e.g., Delazer et al., 2003; Dehaene et al., 2003) as disconnected voxels ranging from the AG to left temporal areas led to impaired arithmetic fact retrieval. However, the region-to-region analyses revealed that not only left AG connectivity but also connectivity of the left and right parietal lobes, as well as further left-hemispheric areas, such as the thalamus, seems to be necessary for the successful retrieval of arithmetic facts. As regards the role of the AG in the fact retrieval network, we suggest that the left AG may not be the (sole) storage location of arithmetic facts. Instead, it may serve a more regulatory role within the network, for instance, subserving semantic integration of concepts (Amalric & Dehaene, 2017; Price et al., 2015) or strategy switching (Bloechle et al., 2016). For instance, patients who could not solve tasks via arithmetic fact retrieval may have had to switch to a different strategy requiring increased magnitude processing (e.g., Dehaene et al., 2003; Klein et al., 2016). If these processing routes to the IPS of either hemisphere were also disconnected (i.e., due to a lesion affecting both association and commissural fibers), patients might not have been able to use this compensatory mechanism adequately. Consequentially, they committed errors or took longer than the ten-second cut-off time to solve the task.

It has been argued that, even within multiplication tasks, there is a size effect, leading to a difference between tasks with multipliers over 5 and those with multipliers under 5 (see Zbrodoff & Logan, 2005). Similarly, Salillas et al. (2012) suggest that in difficult tasks only, TMS disruption of the vertical IPS bilaterally could increase reaction times in a multiplication task. Yet, as we used a standardised subscale from the well-established NPC battery (Delazer et al., 2003), which is based on accuracy measures on a strictly limited number of items (i.e., 36 for arithmetic fact retrieval), effects of problem size in multiplication cannot be evaluated in the current data. Therefore, future work would be desirable to explicitly address the potential effects of problem size in arithmetic fact retrieval with tools better balanced for stimulus magnitude and difficulty.

Conclusion

Our data on lesion-disconnection analyses in unilateral stroke patients suggest that a deficit in arithmetic fact retrieval cannot be tracked to a single locus within the brain. Instead, impairments in arithmetic fact retrieval seem to originate from disconnections of several areas within a (mostly) left-hemispheric network around parietal areas such as the AG, thalamus, STS, STG, MTG and IFG. Interestingly, in both addition and subtraction, patients' performance was very close to ceiling level, indicating that these disconnections may be detrimental specifically to multiplication fact retrieval. Yet, it has to be noted that this is only an indirect inference as it was not possible to analyse associations of disconnections and addition/subtraction performance explicitly due to the lack of variance in the performance data. Therefore, future research would be desirable to test these tasks more specifically. On a more general level, our study underlines the relevance of future research, taking into account grey matter integrity and white matter connectivity in numerical cognition and cognition in general.

References

Amalric, M., & Dehaene, S. (2016). Origins of the brain networks for advanced mathematics in expert mathematicians. *Proceedings of the National Academy of Sciences*, *113*(18), 4909-4917.

Amalric, M., & Dehaene, S. (2017). Cortical circuits for mathematical knowledge: evidence for a major subdivision within the brain's semantic networks. *Philosophical Transactions of the Royal Society B: Biological Sciences*, 373(1740), 20160515.

Amalric, M., & Dehaene, S. (2019). A distinct cortical network for mathematical knowledge in the human brain. *NeuroImage*, 189, 19-31.

Arsalidou, M., Pawliw-Levac, M., Sadeghi, M., & Pascual-Leone, J. (2018). Brain areas associated with numbers and calculations in children: Meta-analyses of fMRI studies. *Developmental Cognitive Neuroscience*, 30, 239-250.

Arsalidou, M., & Taylor, M. J. (2011). Is 2+ 2= 4? Meta-analyses of brain areas needed for numbers and calculations. *NeuroImage*, *54*(3), 2382-2393.

Biniek, R., Huber, W., Glindemann, R., Willmes, K., & Klumm, H. (1992). The Aachen Aphasia Bedside Test--criteria for validity of psychologic tests. *Der Nervenarzt*, *63*(8), 473-479.

Bloechle, J., Huber, S., Bahnmueller, J., Rennig, J., Willmes, K., Cavdaroglu, S., ... & Klein, E. (2016). Fact learning in complex arithmetic—the role of the angular gyrus revisited. *Human Brain Mapping*, *37*(9), 3061-3079.

Brant-Zawadzki, M., Atkinson, D., Detrick, M., Bradley, W. G., & Scidmore, G. (1996). Fluid-attenuated inversion recovery (FLAIR) for assessment of cerebral infarction: initial clinical experience in 50 patients. *Stroke*, 27(7), 1187-1191.

Cohen, L., Dehaene, S., Chochon, F., Lehericy, S., & Naccache, L. (2000). Language and calculation within the parietal lobe: a combined cognitive, anatomical and fMRI study. *Neuropsychologia*, *38*(10), 1426-1440.

de Haan, B., Clas, P., Juenger, H., Wilke, M., & Karnath, H. O. (2015). Fast semi-automated lesion demarcation in stroke. *NeuroImage: Clinical*, 9, 69-74.

Dehaene, S., & Cohen, L. (1995). Towards an anatomical and functional model of number processing. *Mathematical cognition*, 1(1), 83-120.

Dehaene, S., & Cohen, L. (1997). Cerebral pathways for calculation: Double dissociation between rote verbal and quantitative knowledge of arithmetic. *Cortex*, 33(2), 219-250.

Dehaene, S., Piazza, M., Pinel, P., & Cohen, L. (2003). Three parietal circuits for number processing. *Cognitive neuropsychology*, 20(3-6), 487-506.

Delazer, M., Domahs, F., Bartha, L., Brenneis, C., Lochy, A., Trieb, T., & Benke, T. (2003). Learning complex arithmetic—an fMRI study. *Cognitive Brain Research*, *18*(1), 76-88.

Delazer, M., Ischebeck, A., Domahs, F., Zamarian, L., Koppelstaetter, F., Siedentopf, C. M., Kaufmann, L., Benke, T., & Felber, S. (2005). Learning by strategies and learning by drill—evidence from an fMRI study. *NeuroImage*, *25*(3), 838-849.

Delazer, M., Zamarian, L., Benke, T., Wagner, M., Gizewski, E. R., & Scherfler, C. (2019). Is an intact hippocampus necessary for answering 3× 3?–Evidence from Alzheimer's disease. *Brain and Cognition*, *134*, 1-8.

Fan, L., Li, H., Zhuo, J., Zhang, Y., Wang, J., Chen, L., ... & Jiang, T. (2016). The human brainnetome atlas: a new brain atlas based on connectional architecture. *Cerebral Cortex*, *26*(8), 3508-3526.

Gauthier, L., Dehaut, F., & Joanette, Y. (1989). The bells test: a quantitative and qualitative test for visual neglect. *International Journal of Clinical Neuropsychology*, *11*(2), 49-54.

Grabner, R. H., Ansari, D., Koschutnig, K., Reishofer, G., Ebner, F., & Neuper, C. (2009a). To retrieve or to calculate? Left angular gyrus mediates the retrieval of arithmetic facts during problem solving. *Neuropsychologia*, *47*(2), 604-608.

Grabner, R. H., Ischebeck, A., Reishofer, G., Koschutnig, K., Delazer, M., Ebner, F., & Neuper, C. (2009b). Fact learning in complex arithmetic and figural- spatial tasks: The role of the angular gyrus and its relation to mathematical competence. *Human Brain Mapping*, *30*(9), 2936-2952.

Griffis, J. C., Metcalf, N. V., Corbetta, M., & Shulman, G. L. (2019). Structural disconnections explain brain network dysfunction after stroke. *Cell reports*, *28*(10), 2527-2540.

Griffis, J. C., Metcalf, N. V., Corbetta, M., & Shulman, G. L. (2021). Lesion Quantification Toolkit: A MATLAB software tool for estimating grey matter damage and white matter disconnections in patients with focal brain lesions. *NeuroImage: Clinical*, 102639.

Hawes, Z., Sokolowski, H. M., Ononye, C. B., & Ansari, D. (2019). Neural underpinnings of numerical and spatial cognition: An fMRI meta-analysis of brain regions associated with symbolic number, arithmetic, and mental rotation. *Neuroscience & Biobehavioral Reviews*, 103, 316-336.

Hittmair-Delazer, M., Semenza, C., & Denes, G. (1994). Concepts and facts in calculation. *Brain*, *117*(4), 715-728.

Ischebeck, A., Zamarian, L., Siedentopf, C., Koppelstätter, F., Benke, T., Felber, S., & Delazer, M. (2006). How specifically do we learn? Imaging the learning of multiplication and subtraction. *NeuroImage*, *30*(4), 1365-1375.

Ischebeck, A., Zamarian, L., Egger, K., Schocke, M., & Delazer, M. (2007). Imaging early practice effects in arithmetic. *NeuroImage*, *36*(3), 993-1003.

Johannsen, L., & Karnath, H. O. (2004). How efficient is a simple copying task to diagnose spatial neglect in its chronic phase?. *Journal of Clinical and Experimental Neuropsychology*, *26*(2), 251-256.

Johnson, M. D., & Ojemann, G. A. (2000). The role of the human thalamus in language and memory: evidence from electrophysiological studies. *Brain and Cognition*, *42*(2), 218-230.

Kalbe, E., Reinhold, N., Brand, M., Markowitsch, H. J., & Kessler, J. (2005). A new test battery to assess aphasic disturbances and associated cognitive dysfunctions—German normative data on the aphasia check list. *Journal of Clinical and Experimental Neuropsychology*, *27*(7), 779-794.

Kimberg, D. Y., Coslett, H. B., & Schwartz, M. F. (2007). Power in voxel-based lesion-symptom mapping. *Journal of Cognitive Neuroscience*, 19(7), 1067-1080.

Klein, E., Bahnmueller, J., Mann, A., Pixner, S., Kaufmann, L., Nuerk, H. C., & Moeller, K. (2013a). Language influences on numerical development—Inversion effects on multi-digit number processing. *Frontiers in Psychology*, *4*, 480.

Klein, E., Moeller, K., Glauche, V., Weiller, C., & Willmes, K. (2013b). Processing pathways in mental arithmetic—evidence from probabilistic fiber tracking. *PloS One*, *8*(1), e55455.

Klein, E., Moeller, K., & Willmes, K. F. (2013c). A neural disconnection hypothesis on impaired numerical processing. *Frontiers in Human Neuroscience*, *7*, 663.

Klein, E., Suchan, J., Moeller, K., Karnath, H. O., Knops, A., Wood, G., ... & Willmes, K. (2016). Considering structural connectivity in the triple code model of numerical cognition: differential connectivity for magnitude processing and arithmetic facts. *Brain Structure and Function*, *221*(2), 979-995.

Klein, E., Willmes, K., Bieck, S. M., Bloechle, J., & Moeller, K. (2019). White matter neuro-plasticity in mental arithmetic: Changes in hippocampal connectivity following arithmetic drill training. *Cortex*, *114*, 115-123.

Koyama, M. S., Molfese, P. J., Milham, M. P., Mencl, W. E., & Pugh, K. R. (2020). Thalamus is a common locus of reading, arithmetic, and IQ: Analysis of local intrinsic functional properties. *Brain and Language*, 209, 104835.

Lee, K. M. (2000). Cortical areas differentially involved in multiplication and subtraction: a functional magnetic resonance imaging study and correlation with a case of selective acalculia. *Annals of Neurology: Official Journal of the American Neurological Association and the Child Neurology Society*, *48*(4), 657-661.

Lee, M. D., & Wagenmakers, E.-J. (2013). *Bayesian cognitive modeling: A practical course.* Cambridge University Press.

Mah, Y. H., Husain, M., Rees, G., & Nachev, P. (2014). Human brain lesion-deficit inference remapped. *Brain*, 137(9), 2522-2531.

Matejko, A. A., & Ansari, D. (2015). Drawing connections between white matter and numerical and mathematical cognition: a literature review. *Neuroscience & Biobehavioral Reviews*, 48, 35-52.

McCloskey, M., Aliminosa, D., & Sokol, S. M. (1991). Facts, rules and procedures in normal calculation: Evidence from multiple single-patient studies of impaired arithmetic fact retrieval. *Brain and cognition*, *17*(2), 154-203.

Mihulowicz, U., Willmes, K., Karnath, H. O., & Klein, E. (2014). Single-digit arithmetic processing—anatomical evidence from statistical voxel-based lesion analysis. *Frontiers in Human Neuroscience*, *8*, 286.

Moeller, K., Willmes, K., & Klein, E. (2015). A review on functional and structural brain connectivity in numerical cognition. *Frontiers in Human Neuroscience*, *9*, 227.

Noguchi, K., Ogawa, T., Inugami, A., Fujita, H., Hatazawa, J., Shimosegawa, E., ... & Seto, H. (1997). MRI of acute cerebral infarction: a comparison of FLAIR and T2-weighted fast spin-echo imaging. *Neuroradiology*, 39(6), 406-410.

Nichols, T. E., & Holmes, A. P. (2002). Nonparametric permutation tests for functional neuroimaging: a primer with examples. *Human Brain Mapping*, 15(1), 1-25.

Peters, L., & De Smedt, B. (2018). Arithmetic in the developing brain: A review of brain imaging studies. *Developmental Cognitive Neuroscience*, 30, 265-279.

Prado, J., Mutreja, R., Zhang, H., Mehta, R., Desroches, A. S., Minas, J. E., & Booth, J. R. (2011). Distinct representations of subtraction and multiplication in the neural systems for numerosity and language. *Human Brain Mapping*, *32*(11), 1932-1947.

Price, A. R., Bonner, M. F., Peelle, J. E., Grossman, M. (2015) Converging evidence for the neuroanatomic basis of combinatorial semantics in the angular gyrus. *J Neurosci* 35, 3276 – 3284.

Price, C. J. (2012). A review and synthesis of the first 20 years of PET and fMRI studies of heard speech, spoken language and reading. *NeuroImage*, *62*(2), 816-847.

R Core Team (2022). R: A language and environment for statistical computing. R Foundation for Statistical Computing, Vienna, Austria. URL https://www.R-project.org/

Ricci, P. E., Burdette, J. H., Elster, A. D., & Reboussin, D. M. (1999). A comparison of fast spin-echo, fluid-attenuated inversion-recovery, and diffusion-weighted MR imaging in the first 10 days after cerebral infarction. *American Journal of Neuroradiology*, 20(8), 1535-1542.

Rickard, T. C., Romero, S. G., Basso, G., Wharton, C., Flitman, S., & Grafman, J. (2000). The calculating brain: an fMRI study. *Neuropsychologia*, *38*(3), 325-335.

Rorden, C., Bonilha, L., Fridriksson, J., Bender, B., & Karnath, H. O. (2012). Age-specific CT and MRI templates for spatial normalization. *NeuroImage*, 61(4), 957-965.

Rorden, C., & Karnath, H. O. (2004). Using human brain lesions to infer function: a relic from a past era in the fMRI age?. *Nature Reviews Neuroscience*, 5(10), 812-819.

Rorden, C., & Karnath, H. O. (2010). A simple measure of neglect severity. *Neuropsychologia*, *48*(9), 2758-2763.

Saalmann, Y. B., & Kastner, S. (2015). The cognitive thalamus. *Frontiers in Systems Neuroscience*, 9, 39.

Saur, D., Kreher, B. W., Schnell, S., Kümmerer, D., Kellmeyer, P., Vry, M. S., ... & Weiller, C. (2008). Ventral and dorsal pathways for language. *Proceedings of the National Academy of Sciences*, 105(46), 18035-18040.

Schaefer, P. W., Hunter, G. J., He, J., Hamberg, L. M., Sorensen, A. G., Schwamm, L. H., ... & Gonzalez, R. G. (2002). Predicting cerebral ischemic infarct volume with diffusion and perfusion MR imaging. *American Journal of Neuroradiology*, 23(10), 1785-1794.

Sperber, C., Griffis, J., & Kasties, V. (2022). Indirect structural disconnection-symptom mapping. *Brain Structure and Function*, in press, 1-16.

Sperber, C., & Karnath, H. O. (2017). Impact of correction factors in human brain lesion-behavior inference. *Human Brain Mapping*, 38(3), 1692-1701.

van Harskamp, N. J., & Cipolotti, L. (2001). Selective impairments for addition, subtraction and multiplication. Implications for the organization of arithmetical facts. *Cortex*, *37*(3), 363-388.

Van Harskamp, N. J., Rudge, P., & Cipolotti, L. (2005). Cognitive and social impairments in patients with superficial siderosis. *Brain*, *128*(5), 1082-1092.

Weber, J., Mattle, H. P., Heid, O., Remonda, L., & Schroth, G. (2000). Diffusion-weighted imaging in ischaemic stroke: a follow-up study. *Neuroradiology*, 42(3), 184-191.

Weiller, C., Bormann, T., Saur, D., Musso, M., & Rijntjes, M. (2011). How the ventral pathway got lost–And what its recovery might mean. *Brain and Language*, 118(1-2), 29-39.

Weintraub, S. (1985). Mental state assessment of young and elderly adults in behavioral neurology. *Principles of Behavioral Neurology*, 71-123.

Wetzels, R., & Wagenmakers, E. J. (2012). A default Bayesian hypothesis test for correlations and partial correlations. *Psychonomic Bulletin & Review*, 19(6), 1057-1064.

Willmes, K., Moeller, K., & Klein, E. (2014). Where numbers meet words: a common ventral network for semantic classification. *Scandinavian Journal of Psychology*, 55(3), 202-211.

Yeh, F. C., Panesar, S., Fernandes, D., Meola, A., Yoshino, M., Fernandez-Miranda, J. C., ... & Verstynen, T. (2018). Population-averaged atlas of the macroscale human structural connectome and its network topology. *NeuroImage*, *178*, 57-68.

Zamarian, L., Ischebeck, A., & Delazer, M. (2009). Neuroscience of learning arithmetic—evidence from brain imaging studies. *Neuroscience & Biobehavioral Reviews*, *33*(6), 909-925.

Zamarian, L., Karner, E., Benke, T., Donnemiller, E., & Delazer, M. (2006). Knowing 7× 8, but not the meaning of 'elephant': evidence for the dissociation between numerical and non-numerical semantic knowledge. *Neuropsychologia*, 44(10), 1708-1723.

Zaunmüller, L., Domahs, F., Dressel, K., Lonnemann, J., Klein, E., Ischebeck, A., & Willmes, K. (2009). Rehabilitation of arithmetic fact retrieval via extensive practice: a combined fMRI and behavioural case-study. *Neuropsychological Rehabilitation*, *19*(3), 422-443.

Zbrodoff, N. J. & Logan, G. D. (2005). What Everyone Finds: The Problem-Size Effect. In Campbell, J. I. (Ed.) *The Handbook of Mathematical Cognition* (pp. 349-364). Psychology Press.

Appendix

Appendix A:

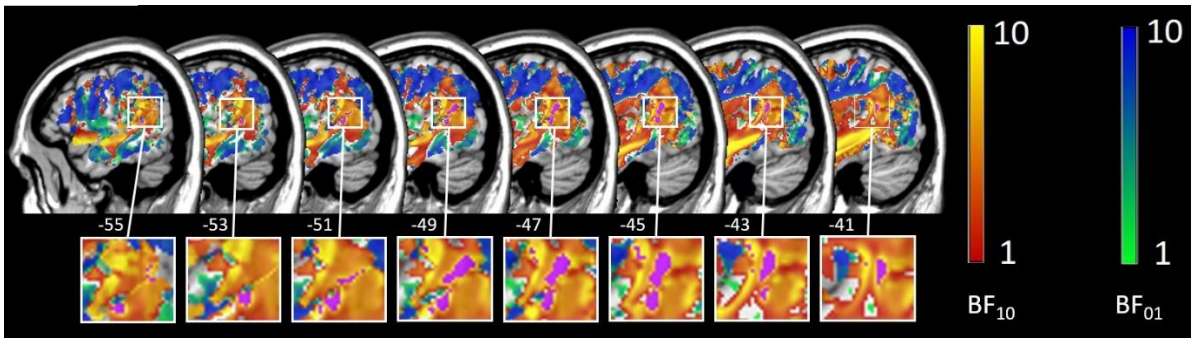

FIGURE 4 | Bayesian disconnectivity mapping after exclusion. Sagittal View of the left hemisphere. The heatmap denotes Bayes factors of correlations between voxel-wise disconnection value and multiplication score. Voxels marked in a red-to-yellow manner had BFs indicating evidence for their association with multiplication score, while voxels marked in green-to-blue indicate evidence for no association with multiplication score. Purple indicates the voxels that were significant following the frequentist analysis (see Figure 2). The sagittal x-coordinate of standardized MNI space is given below each slice. Note that in this image the scale starts at 1, as no logarithms are displayed.

Competing interests

911 The authors have no competing interests to disclose.

912

913 # AcknowledgementsF

914 This work was supported by the Deutsche Forschungsgemeinschaft (KL 2788/2-1 und KA
915 1258/24-1). We thank all patients who participated in this study as well as the nursing staff of
916 the University of Tuebingen who assisted with patient preparation.

Data and Code Availability Statement

Online materials, including all analysis scripts, descriptive data, and resulting topographies, are publicly available at http://dx.doi.org/10.17632/yjkr647mzb.1. The clinical datasets analyzed in the current study are not publicly available due to the data protection agreement approved by the local ethics committee and signed by the participants.